Magnetism of 3*d* transition-metal monolayers and two-dimensional Cr clusters deposited on Fe(001)

Laurent Pizzagalli, D. Stoeffler, and F. Gautier
Institut de Physique et de Chimie des Matériaux de Strasbourg, Groupe d'Etude des Matériaux Métalliques (UMR 46 CNRS-ULP-EHICS), 23 rue du Loess, 67037 Strasbourg, France
(Received 4 March 1996; revised manuscript received 1 July 1996)

We study the magnetic properties of transition-metal monolayers (ML) and Cr clusters deposited on Fe(001). We use a self-consistent tight-binding model and the recursion technique in order to get the most stable magnetic state for each atomic configuration. The magnetism is taken into account in the mean-field approximation. We show that for a Cr ML the $p(2\times2)$ magnetic solution is lower in energy than all the others. We find that monolayers of V, Ni, and Co are ferromagnetic $p(1\times1)$ on Fe(001) whereas the Mn ML are $c(2\times2)$ antiferromagnetic. We study also the magnetic transition occurring for Cr clusters, for an increasing Cr atoms number, from ferromagnetic to the $p(2\times2)$ order. The results of these calculations are in agreement with those of an Ising model whose parameters are determined. Such an Ising model predicts with a good accuracy the most stable state and the first excited states for each cluster shape. [S0163-1829(96)04942-9]

I. INTRODUCTION

The study of the magnetic properties of surfaces, thin films, and superlattices is now a very active field of research in relation to the improvement of the magnetic recording. This has led to an increasing number of experimental and theoretical studies, particularly for transition-metal systems. Even if the understanding of effects such as the giant magnetoresistance and the oscillatory interlayer couplings in the multilayers has significantly progressed, a lot of theoretical and experimental work remains to be done to understand the relation between the interfacial structure and the corresponding magnetic properties. The Cr/Fe system is a good example of such a problem. It has been extensively studied both theoretically[1–6] and experimentally,[7–14] in relation with the properties of the corresponding multilayers. However, the whole understanding of these properties is far from being realized.

A first tight-binding study of Allan[15] has pointed out that a chromium (001) surface would exhibit a large magnetic moment of $2.8\mu_B$, which represents a very large enhancement as compared with the bulk magnetic moment value ($0.59\mu_B$). Consequently, a large number of works has been devoted to the investigation of Cr deposited on ferromagnets. Until recently, all the theoretical investigations of a Cr monolayer (ML) deposited on a Fe substrate were based on the assumption that the Cr monolayer is ferromagnetically ordered $[p(1\times1)]$. This assumption seems natural if we consider the Cr bulk magnetism which is driven by an incommensurable spin-density wave (SDW) in the (001) direction of approximately 21 lattice spacings wavelength.[16] This SDW yields approximately a layered antiferromagnetic structure where alternated planes carry opposite magnetic moments. Therefore, the (001) surface plane is expected to be ferromagnetically ordered[3,15,17–20] and a Cr ML deposited on Fe(001) is also thought to be ferromagnetically ordered and antiferromagnetically (AF) coupled to Fe. In this scheme, the self-consistent tight-binding calculations of Victoria and co-workers[1,3] found a giant Cr magnetic moment of $3.65\mu_B$ whereas *ab initio* full-potential linearized augmented-plane-wave (FLAPW) calculations by Fu, Freeman, and Oguchi found $3.1\mu_B$.[2] More recent tight-binding studies[4,5] found Cr magnetic moments of 2.5 and $3.2\mu_B$.

However, if all the theoretical studies agree qualitatively on the values of the predicted moment, there is some disagreement between the corresponding experimental investigations and also between the experimental and the theoretical results. For example, (i) Jungblut *et al.*[8] estimated the Cr moment to be equal to $1\mu_B$ for a ferromagnetic Cr monolayer coupled AF with Fe, (ii) a spin-polarized electron-energy-loss spectroscopy study by Walker *et al.*[9] measured a Cr surface exchange splitting of 1.9 eV, indicating a very large magnetic moment, and (iii) Idzerda *et al.*[11] deduced the magnetic moment value from soft-x-ray magnetic circular dichroism measurements and found $0.6\mu_B$ for a Cr coverage equal to 0.25. Finally, a recent and controversial experience[12] using an *in situ* magnetometry technique determined a magnetic moment larger than $3\mu_B$. Several authors have tried to explain this disagreement. From an experimental point of view, the Cr magnetism is highly sensitive to the structure of the interfaces and to the growth mode as suggested by the study of Cr/Fe(001) and the coupling of the Fe layers between a Cr layer. Moreover, the Cr magnetism is extremely sensitive to the contamination and there can be doubts about the cleanliness of the Cr/Fe samples. From a theoretical point of view, Blügel, Weinert, and Dederichs suggested that the in-plane antiferromagnetic order $[c(2\times2)]$ could be the most stable one. The full-potential linearized augmented-plane-wave (FLAPW) calculations showed that this solution is more stable than the $p(1\times1)$ one for a Cr free-standing ML and Cr monolayers deposited on Pd(001), Ag(001), and Au(001) substrates,[21] whereas the $p(1\times1)$ order is the most stable one for the Cr(001) surface.[22] The tight-binding calculations by Vega *et al.*[6] found that the $c(2\times2)$ solution is energetically lower than $p(1\times1)$ for a Cr ML deposited on Fe(001) but such discrepancies can be understood if we note that the energy differences between these solutions are small.

In this paper, we investigate the possible magnetic con-

figurations for the 3d transition metal ML on Fe(001) and for some Cr clusters deposited on Fe(001). We use a self-consistent tight-binding model to determine the ground states for the considered atomic configurations. We show that these results are consistent with those of an Ising model which allows us to get magnetic phase diagrams. Section II is devoted to a brief description of the tight-binding model and of the parameters we use. Section III summarizes our results for the adsorbed monolayers. Surprisingly, we show that a new ferrimagnetic solution, the $p(2\times2)$ structure, is the most stable one for Cr/Fe(001). In Sec. IV, we study the Cr magnetic transitions which must occur when very small ferromagnetic clusters (3 or 4 adatoms) grow and become ferrimagnetic. We suggest that such a transition can explain the magnetism of ultrathin layers in relation with their growth. We show that an Ising model is well suited for this investigation and predict with a good accuracy the magnetic transition. Hence, a systematic study of small two-dimensional (2D) Cr clusters is presented in Sec. V. We conclude in Sec. VI.

II. TIGHT-BINDING MODEL

In this paper, the electronic-structure calculations have been done within the tight-binding scheme. The *ab initio* method is the most accurate one for the monolayer/substrate system, i.e., for a system for which the number of inequivalent atoms on which self-consistency have to be realized is small. However, in Sec. IV, we investigate large Cr clusters with 400 adatoms and the number of inequivalent atoms in such calculations is too large ($\simeq$1100) for these approaches. For example, Wildberger *et al.*,[23] in a recent *ab initio* study, investigated at most nine adatoms clusters.

We use the tight-binding approximation because for transition metals, the cohesion is mostly ensured by itinerant d electrons. The sp electrons are not taken into account here. Their influence on the magnetic properties has been shown to be negligible.[24–26] In the localized orbitals basis $|i,\lambda,\sigma\rangle$ (site i, symmetry λ, spin σ), the one-electron tight-binding Hamiltonian can be written as

$$H=\sum_{i,\lambda,\sigma}|i,\lambda,\sigma\rangle\epsilon_i^{\sigma}\langle\sigma,\lambda,i|+\sum_{\substack{i,j\neq i\\ \lambda,\mu\neq\lambda,\sigma}}|i,\lambda,\sigma\rangle\beta_{ij}^{\lambda\mu}\langle\sigma,\mu,j|. \tag{1}$$

The diagonal term ϵ_i^{σ} is the intrasite energy level and the off-diagonal term $\beta_{ij}^{\lambda\mu}$ is the intersite hopping integral. Several approximations[27] have been made here: (i) The small crystalline field integrals have been neglected, (ii) the basis set of atomic orbitals have been assumed to be orthonormalized, and (iii) only the two-center hopping integrals for nearest and next-nearest neighbors are considered and are expressed from three parameters $dd\sigma, dd\pi, dd\delta$, which are only dependent of the bandwidth. Here, we use

$$(dd\sigma, dd\pi, dd\delta)=(6,-4,1)dd\delta, \tag{2}$$

$dd\delta$ is chosen to get the bulk bandwidth (7.26 eV for Cr and 5.34 eV for Fe). We assume that these integrals are spin independent and vary a power law d^{-5} versus the interatomic distance d. In the case of hopping integrals between one Cr atom and one Fe atom, we use the Shiba approximation[28]

$$\beta_{\text{Cr-Fe}}^{\lambda\mu}=\sqrt{\beta_{\text{Cr-Cr}}^{\lambda\mu}\beta_{\text{Fe-Fe}}^{\lambda\mu}}. \tag{3}$$

We assume that the crystalline structure of the adsorbed ML is cubic and in perfect epitaxy with the iron (001) surface. Moreover, in our calculations, we do not take into account the relaxation of the adsorbate relative to the Fe substrate. The total band energy for the given Hamiltonian is

$$E_b=\sum_{i,\sigma}\int_{-\infty}^{\epsilon_F}\epsilon n_{i,\sigma}(\epsilon)d\epsilon. \tag{4}$$

$n_{i,\sigma}(\epsilon)$ is the local density of state on site i and the spin $\sigma=+1$ or -1 which we calculate with the recursion method[29–31] and the Beer-Pettifor[32] termination. The continuous fraction is expanded up to the eighth exact level. We verified that extra levels provide negligible variations on the values of the magnetic moments.

Charge transfers must occur in the vicinity of defects such as surfaces. We add the variation of the Coulomb term to the variation of the band energy to account for this electronic rearrangement. The Coulomb correction relative to the bulk value E_C^0 is given by

$$\delta E_C=-\sum_{i,\lambda}(N_{i,\lambda}+\tfrac{1}{2}\,\delta N_{i,\lambda})\,\delta V_i, \tag{5}$$

where δV_i is the symmetry-independent variation of the Coulomb potential on site i, $N_{i,\lambda}$ is the band occupation for the symmetry λ on site i, and $\delta N_{i,\lambda}$ its variation. Here we use the local neutrality approximation ($\Sigma_\lambda\delta N_{i,\lambda}=0$):

$$\delta E_C=-\sum_i N_i\delta V_i, \tag{6}$$

which is valid when the difference between the various energy levels is small. Magnetism effects are treated in the mean-field approximation. The up and down spin are separated by the shift Δ_i and the magnetic moment M_i is proportional to the difference between the two local spin subband occupations. The self-consistent relation is given by

$$\Delta_i=M_i\cdot I, \tag{7}$$

where I is the effective exchange integral. Here we used $I_{\text{V}}=0.42$ eV, $I_{\text{Cr}}=0.558$ eV, $I_{\text{Mn}}=0.587$ eV, $I_{\text{Fe}}=0.618$ eV, $I_{\text{Co}}=0.82$ eV, and $I_{\text{Ni}}=0.85$ eV in order to recover the bulk magnetic moments $M_{\text{Cr}}=0.6\mu_B$ and $M_{\text{Mn}}=2.5\mu_B$ for antiferromagnetic Cr and Mn, $M_{\text{Fe}}=2.2\mu_B$, $M_{\text{Co}}=1.76\mu_B$, and $M_{\text{Ni}}=0.6\mu_B$ for ferromagnetic Fe, Co, and Ni. A magnetic double counting energy correction is added to the band energy, the total energy becomes

$$E=\sum_{i,\sigma}\int_{-\infty}^{\epsilon_F}\epsilon n_{i,\sigma}(\epsilon)d\epsilon-\sum_i\left(N_i\delta V_i+\frac{I_iM_i^2}{4}\right)+E_C^0. \tag{8}$$

The self-consistent calculations are done on a given site, the other values of ϵ_i^{σ} being unchanged. We repeat this process for all sites until convergence is realized. Details of this procedure can be found elsewhere.[5] Self-consistency is required on n inequivalent sites, n being dependent of the system under study. For a Cr monolayer deposited on Fe(001), we consider eight first Fe layers [$n=19$ for a $p(2\times2)$ con-

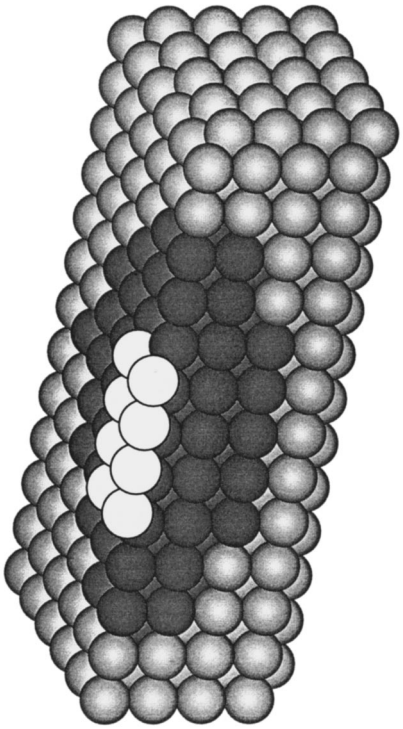

FIG. 1. Section of a system made of a 16 adatoms square cluster (white circles) deposited on a bcc (001) surface (gray circles). Self-consistent calculations are done on each of the cluster adatoms (white circles) and of the substrate atoms located in a semiellipsoid centered on the cluster (dark gray circles) whereas other atoms (light gray circles) are assumed to be nonperturbed by the cluster adsorption. We verified that the perturbed and nonperturbed atoms have nearly the same electronic structure and magnetic properties at the boundaries of the ellipsoid we choose.

figuration for example]. In the case of a Cr cluster, the in-plane periodicity is broken. Calculations must be done on all cluster sites and on all substrate sites perturbed by the adsorption. The criterion we use to choose n is that the sites which are the most apart from the perturbation have the same properties as the nonperturbed sites. In practice, we require self-consistency on sites located inside a semiellipsoid centered on the cluster (Fig. 1). For example, we studied the adsorption of a 400 adatoms cluster, involving about 1100 inequivalent sites.

We determine the most stable state between two different magnetic configurations by comparing the calculated energies [Eq. (8)]. The Ising interaction parameters are deduced from these energy differences. Note that we do not take into account the repulsive energy needed for the crystal cohesion, since it is not modified by the magnetism for a given atomic configuration. Finally, we assume, in this paper, that all magnetic moments are collinear.[5]

III. MONOLAYERS

Most of the theoretical studies concerning the magnetism of a monolayer deposited on a substrate dealt only with the $p(1\times1)$ ferromagnetic and the $c(2\times2)$ ferrimagnetic solutions. However, the magnetic ground state can be more complicated. We cannot investigate all the possible magnetic

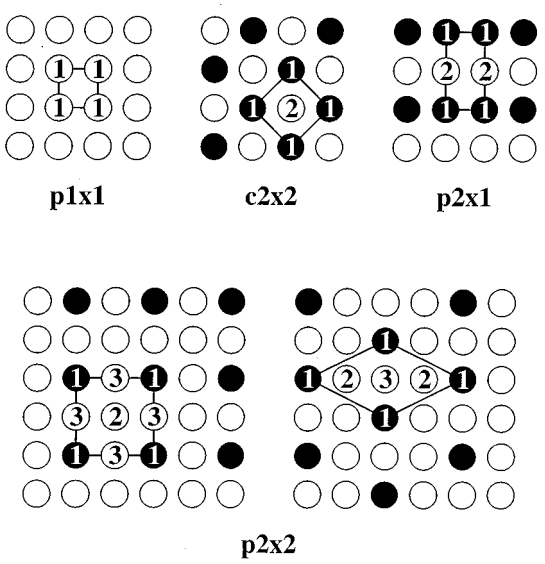

FIG. 2. Some possible magnetic configurations of the monolayer. Black and white circles represent positive and negative spins. The numbers inside the circles of the periodic cell label the inequivalent atoms. For the $p(2\times2)$ structure, we show the two simplest arrangements although among all the possible ones. The configuration represented at the left of the figure is referred as $p(2\times2)_\alpha$ whereas the other one is labeled $p(2\times2)_\beta$. Note that for solutions which are noninvariant when we change the sign of the adsorbates magnetic moments, such $p(1\times1)$ [or $p(2\times2)$], we must consider one configuration with more spins up and another with more spins down.

configurations from an electronic structure point of view. This is why, anticipating the mapping of the tight-binding calculations on the Ising model results, we restrict our study to those states which are stable in an Ising model assuming that only nearest and next-nearest in-plane neighbors (second and third neighbors in the bulk) interactions are nonzero. Considering the precision of the tight-binding model, it is obvious that the study of more complex magnetic orders involving very small energy differences is out of reach. With the previous limitations, we considered four types of magnetic configurations (Fig. 2): (i) the usual $p(1\times1)$ and $c(2\times2)$, (ii) the $p(2\times1)$ where ferromagnetic rows are alternated antiferromagnetically, and (iii) a more complex $p(2\times2)$ structure. The $p(2\times1)$ and $c(2\times2)$ configurations are symmetric since they include as many spins up as spins down whereas $p(1\times1)$ and $p(2\times2)$ are not. According to the sign of the adsorbate-Fe coupling, one can have $p(1\times1)$ and $p(2\times2)$ configurations with more spins up (F coupled to Fe) or more spins down (AF coupled to Fe). As remarked by Ducastelle,[33] it is possible to build an infinity of structures with the $p(2\times2)$ elementary cell. As an example we study the two simplest possible $p(2\times2)$ configurations (Fig. 2).

Table I shows the magnetic moments and the energy difference between the magnetic configurations. Let us briefly summarize the main results of this study:

(i) For the V ML, only one solution, the $p(1\times1)^{\downarrow}$ one, is obtained where the V magnetic moments are AF coupled with Fe magnetic moments. The V moments are found to be large ($-2.66\mu_B$). This last result is in discrepancy with previous tight-binding calculations[34] predicting a low-spin solu-

tion for $I_V=0.42$ eV. As noted by Bouarab, Khan, and Demangeat the high sensitivity of the magnetism versus the exchange parameter I is a possible explanation.[35]

(ii) The most surprising result is obtained for a Cr ML on Fe(001). We found that the $p(2\times2)^{\downarrow}$ solution is energetically lower than all the others whereas we expected a $c(2\times2)$ ground state.[6,36,37] The energy difference δE between the $p(2\times2)^{\downarrow}$ and $c(2\times2)$ solutions is small (approximately 27 meV/atom) but we think it is significant. On the other hand, there is no doubt that the usual $p(1\times1)^{\downarrow}$ configuration is not the most stable state since in this case δE is 53 meV/atom. We calculated the mean magnetic moment in the surface by averaging the magnetic moments of inequivalent adatoms. We find $-1.91\mu_B$ for the $p(2\times2)^{\downarrow}$ structure. This can explain the experimental results[8,9,11,12] which can only measure a mean surface magnetization. We studied also the two magnetic configurations for which the majority of spins are F coupled with Fe ones. In the first case $[p(1\times1)^{\uparrow}]$ no solution was obtained whereas in the second case $[p(2\times2)^{\uparrow}]$, the resultant magnetic moments are frustrated and are small (approximately $0.5\mu_B$).

(iii) As previously found by Wu and Freeman,[36] the $c(2\times2)$ solution is the most stable state for the Mn/Fe(001) system. In their study, the energy difference between $c(2\times2)$ and $p(1\times1)$ solutions is small (78 meV) whereas we found it is larger than 200 meV. The $c(2\times2)$ buckling reconstruction that they considered can be partially at the origin of this disagreement. Another recent tight-binding study[38] also finds this $c(2\times2)$ solution.

(iv) We thought *a priori* that the Fe/Fe(001) $p(1\times1)^{\uparrow}$ state is the ground state but we discovered that the energy of the $p(2\times2)^{\uparrow}$ is lower. The energy difference is very small (11 meV/atom) and probably of the order of the uncertainty. It would be interesting that further *ab initio* calculations investigate this $p(2\times2)^{\uparrow}$ magnetic configuration. Our results for the calculated $p(1\times1)^{\uparrow}$ magnetic moments agree with others studies.[24,25,39,40]

(v) Co and Ni ML present the same characteristics. A monolayer of Ni or Co deposited on Fe(001) is unambiguously in a $p(1\times1)^{\uparrow}$ magnetic state. All the other possible solutions are numerically unstable, except the $p(1\times1)^{\uparrow}$ solution for Co, the Fe magnetic moment at the interface being AF coupled with others Fe moments. In this case, we can conclude that the F coupling interaction between Co and Fe is stronger that the one between two Fe layers.

From tight-binding or *ab initio* calculations, we get numerical values for several physical quantities but it is often difficult to explain the physical behavior in an easy way. Here, we propose to map the results we found above on those of an Ising model. Basically, within an Ising model, the magnetic energy of a monolayer of a transition metal X deposited on a substrate Y can be written as

$$E_{\mathrm{mag}}=\sum_{i=1}^{N_{\mathrm{ad}}}\left(-\sum_{\langle i,j\rangle}J_1\mathbf{S}_i^X\mathbf{S}_j^Y-\frac{1}{2}\sum_{\langle i,j\rangle}J_2\mathbf{S}_i^X\mathbf{S}_j^X-\frac{1}{2}\sum_{\langle i,j\rangle}J_3\mathbf{S}_i^X\mathbf{S}_j^X\right). \tag{9}$$

The second and third terms on the right-hand side corresponding to the in-plane monolayer interaction energies, for in-plane first (J_2) and second (J_3) neighbors. On the other hand, the first term is only the sum of the interaction energies between X adatoms and Y surface layer first-neighbor atoms. In fact, the formalism is strictly the same as the one we use if we consider a free-standing monolayer with an external applied magnetic field.[33] Physically, the three Ising parameters represent the couplings between two atoms which are either F ($J>0$) or AF ($J<0$). One of the main assumptions of this Ising model is that the amplitude of the moments do not vary with the magnetic configuration, which is not the case in the itinerant magnetism framework. However, Table I shows that the values of most of them are very close to each other when the considered magnetic configurations do not present frustrations. Using the Eq. (9) for the magnetic energy, we can derive the energy differences δE analytically for each magnetic configuration and obtain the parameters J_1, J_2, and J_3 when we get a sufficient number of different magnetic configurations. Figure 3 shows the phase diagram for this system versus $-J_2/|J_1|$ and $-J_3/|J_1|$. The sign of J_1 determines either a F coupling $[p(1\times1)^{\uparrow}, p(2\times2)^{\uparrow}]$ or an AF coupling $[p(1\times1)^{\downarrow}, p(2\times2)^{\downarrow}]$ for nonsymmetric magnetic configurations. Table II shows the J parameters for Cr, Mn, and Fe. It has not been possible to determine J_1 and J_2 for Cr because of the lack of a sufficient number of different magnetic solutions. In fact, we cannot use the $p(2\times1)$ solution since the positive magnetic moment on frustrated adatoms (F coupled with Fe) is too small and the energy values lead to strong numerical errors on the Ising parameters, as seen below.

The Mn-Mn (J_2,J_3) and Fe-Mn (J_1) couplings are all AF. We verified that the Mn ground state is $c(2\times2)$ with $-J_2/|J_1|\simeq5$ and $-J_3/|J_1|\simeq1.7$. The case of a Fe ML is rather different, since the adlayer-substrate Fe-Fe coupling is now F, the intralayer couplings always being AF. We get $-J_2/|J_1|\simeq0.8$ and $-J_3/|J_1|\simeq0.5$, in the $p(2\times2)^{\uparrow}$ region in the phase diagram (Fig. 3), very near to the $p(1\times1)^{\uparrow}$ region. We cannot determine the J parameters for V, Co, and Ni since only one solution is available. J_1 must be much larger than (J_2,J_3), a consequence of the predominance of the $p(1\times1)$ state. Obviously, $J_1<0$ for V and $J_1>0$ for Co and Ni.

We represent in Fig. 4 the energy differences for each magnetic configuration and each element. The magnetic configurations are plotted along the horizontal axis according to the number of spins up, from $p(1\times1)^{\uparrow}$ to $p(1\times1)^{\downarrow}$. One can see clearly that the most stable state changes from one configuration to another one along the transition-metal series. Several major trends can be deduced from Fig. 4 and Table I: (i) $|J_2|$ and $|J_3|$ decrease along the $3d$ series from V to Ni. Their values being negative for Cr, Mn, and Fe, the in-plane magnetic couplings for the first and second neighbors are AF. (ii) The adsorbate-substrate magnetic interaction J_1 is large and negative at the beginning of the series (AF coupling). Then it increases in the middle (Mn,Fe) of the series to become large and positive at the end (F coupling). A set of tight-binding parameters, intermediate between those of Mn and Fe can lead to magnetically decoupled adsorbate ML and substrate. (iii) J_3 is always smaller than J_2 or J_1. The $p(2\times1)$ solution is never the most stable state. Topological defects such as parallel steps may induce such a solution.[4]

TABLE I. Energy differences δE in meV and magnetic moments in μ_B for each magnetic configurations and each system X/Fe(001). δE is the difference for one adlayer atom between this configuration and the most stable one for each system. The numbering of the magnetic moments M_{1-3} refers to the nonequivalent adatoms and M_{Fe} is the Fe interface moment. The missing magnetic configurations for V, Cr, Co, and Ni are numerically instable. Note the strong reduction of the magnetic moment for $p(2\times2)^{\uparrow}$ Cr/Fe(001) and the spin flip of the Fe interface moment for $p(1\times1)^{\downarrow}$ Co/Fe(001).

		δE	M_1	M_2	M_3	M_{Fe}
V	$p(1\times1)^{\downarrow}$	0	−2.66			1.91
Cr	$p(2\times2)^{\downarrow\beta}$	0	3.08	−2.98	−2.92	1.73
	$p(2\times2)^{\downarrow\alpha}$	3	3.10	−3.04	−2.90	1.73
	$c(2\times2)$	27	−2.81	2.72		1.53
	$p(1\times1)^{\downarrow}$	53	−3.19			1.82
	$p(2\times1)$	64	−2.90	2.15		1.51
	$p(2\times2)^{\uparrow\alpha}$	141	−2.82	0.67	0.50	1.37
	$p(2\times2)^{\uparrow\beta}$	141	−2.84	0.74	0.70	1.36
Mn	$c(2\times2)$	0	−3.26	3.15		1.53
	$p(2\times2)^{\downarrow\alpha}$	56	3.12	−3.18	−3.27	1.56
	$p(2\times2)^{\downarrow\beta}$	59	3.16	−3.23	−3.25	1.57
	$p(2\times1)$	59	−3.25	3.22		1.52
	$p(2\times2)^{\uparrow\alpha}$	111	−3.19	3.17	3.16	1.39
	$p(2\times2)^{\uparrow\beta}$	111	−3.19	3.16	3.16	1.39
	$p(1\times1)^{\downarrow}$	207	−3.03			1.64
	$p(1\times1)^{\uparrow}$	311	2.98			1.06
Fe	$p(2\times2)^{\uparrow\beta}$	0	−2.25	2.63	2.55	1.96
	$p(2\times2)^{\uparrow\alpha}$	1	−2.26	2.71	2.52	1.93
	$p(1\times1)^{\uparrow}$	11	2.63			2.05
	$p(2\times1)$	11	−2.25	2.58		1.84
	$c(2\times2)$	27	−2.31	2.37		1.66
	$p(2\times2)^{\downarrow\beta}$	71	2.44	−2.15	−2.26	1.63
	$p(2\times2)^{\downarrow\alpha}$	78	2.44	−2.23	−2.27	1.63
	$p(1\times1)^{\downarrow}$	157	−2.23			1.49
Co	$p(1\times1)^{\uparrow}$	0	1.64			2.60
	$p(1\times1)^{\uparrow}$	153	−1.62			−2.17
Ni	$p(1\times1)^{\uparrow}$	0	0.54			2.76

IV. CLUSTER-MONOLAYER MAGNETIC TRANSITIONS

We concluded in the first section that the most stable state for a Cr monolayer deposited on Fe(001) is not the $p(1\times1)^{\downarrow}$ configuration but the $p(2\times2)^{\downarrow}$ one. Therefore, there must be a magnetic transition inside a 2D cluster when its size increases from a $p(1\times1)^{\downarrow}$ configuration towards the $p(2\times2)^{\downarrow}$ configuration. To our knowledge, it seems that no one has studied such a transition, which is of a great interest in the domain of the evolution of the magnetic properties during the growth. Here, we investigate these magnetic transitions for 2D Cr clusters deposited on Fe(001). Moreover, we will be able to deduce completely the Ising parameters from these calculations.

In practice, we study several magnetic configurations for two cluster types, square-shaped and diamond-shaped, with different sizes, x is the square or diamond side length in lattice parameter a_0 for clusters including $(x+1)^2$ adatoms (square) or $x^2+x\sqrt{2}+1$ adatoms (diamond). We investigate the $p(1\times1)^{\downarrow}$, $c(2\times2)$, $p(2\times2)^{\downarrow}_{\alpha}$ and an hybrid magnetic configuration with AF coupling on the borders atoms of the adsorbate clusters and $c(2\times2)$ magnetic configuration inside

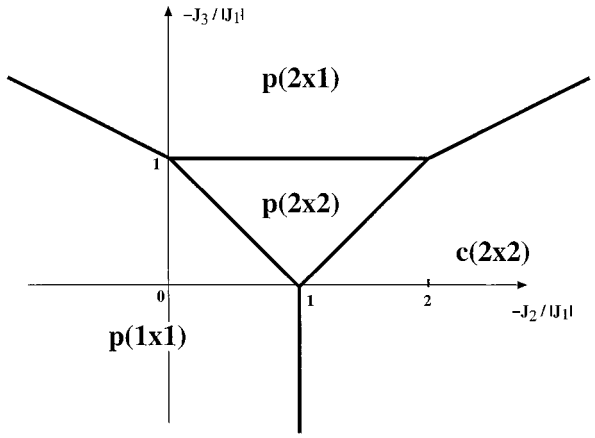

FIG. 3. Phase diagram $(-J_2/|J_1|,-J_3/|J_1|)$ for a monolayer deposited on a substrate or a free-standing monolayer with an external magnetic field (Ising model) (Ref. 33). The sign of J_1 determines the possible solutions, i.e., either $p(1\times1)^{\downarrow}$ and $p(2\times2)^{\downarrow}$ ($J_1 0$) or $p(1\times1)^{\uparrow}$ and $p(2\times2)^{\uparrow}$ ($J_2 0$).

TABLE II. Ising parameters in meV for middle-series elements Cr, Mn, and Fe. In case of Cr, J_1 and J_2 are not determined due to some nonresolved magnetic configurations.

	J_1 (meV)	J_2 (meV)	J_3 (meV)
Cr	$J_1-J_2\simeq 6$		-22
Mn	-13	-64	-22
Fe	18	-14	-9

this cluster (Fig. 5). We calculate the energies increasing x, and compare the three latest ones with the $p(1\times1)^{\downarrow}$ one.

Adatoms which are F magnetically coupled with the Fe substrate are called ''frustrated'' since Cr-Fe couplings are usually AF. We notice that small clusters with less-coordinated frustrated adatoms on their sides are numerically unstable or energetically metastable. We expect gains in energy when only nonfrustrated adatoms are located on the cluster sides as obtained in a $p(1\times1)^{\downarrow}$ scheme. This is why we consider the special magnetic geometry such as the hybrid configuration. On the other hand, we saw that a Cr monolayer deposited on Fe(001) prefers in-plane AF [$p(2\times2)^{\downarrow}_{\alpha}$ or $c(2\times2)$] rather than in-plane F [$p(1\times1)^{\downarrow}$]. To summarize, we expect a side effect proportional to x favoring in-plane F and a surface effect proportional to x^2 favoring in-plane AF. Therefore, we can suggest *a priori* that the following expression:

$$\delta E = E[p(1\times1)^{\downarrow}] - E(\mathrm{AF}) = ax^2 + bx + c \qquad (10)$$

with $a>0$. We checked the validity of this general expression with the Ising model and derived the energy differences for each case (Table III).

Figure 6 shows the total-energy differences in the case of square-shaped and diamond-shaped clusters. The calculated data fit nicely with a quadratic regression, as expected. It is clear that the $p(2\times2)^{\downarrow}$ cluster is energetically lower than all the other configurations, even for very small sizes. On the other hand, 400 adatoms square cluster has been studied in order to get the transition between $p(1\times1)^{\downarrow}$ and $c(2\times2)$. In the case of diamond cluster, we find that the $c(2\times2)$ structure becomes more stable than the $p(1\times1)^{\downarrow}$ one and more quickly than for square clusters. This can be qualitatively understood from the fact that the geometry of these clusters is like a $c(2\times2)$ cell, leaving no frustrated adatoms on the sides. However, the transition is not exactly obtained for $x=0$, as predicted by the Ising expression (Table III). It is rather difficult to get precise results for very small clusters, the Ising model being more suited for larger sizes. With these data and the fitted functions of the Table III; we can easily deduce the three Ising parameters. We get $J_1=-106$ meV, $J_2=-111$ meV, and $J_3=-23$ meV. These values are in agreement with the parameters calculated from the monolayer results. Moreover, the values of J_1 and J_2 confirm the

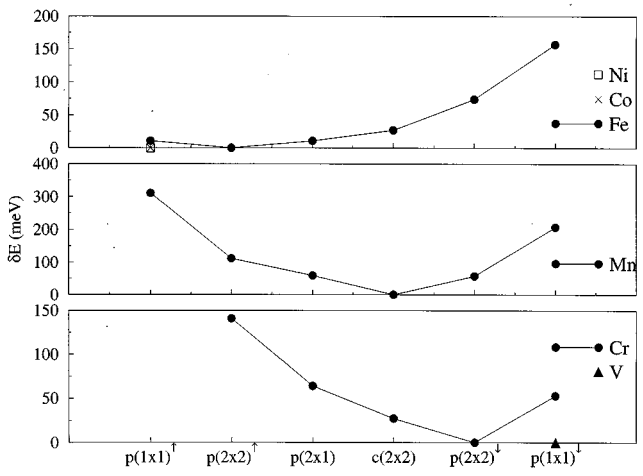

FIG. 4. Energy difference in meV between each magnetic configuration and the most stable one, for each element of the 3d series. The magnetic configurations on the abscissa axis are arranged from left to right increasing the number of spins down. Note the change of the magnetic ground state going from Ni to V.

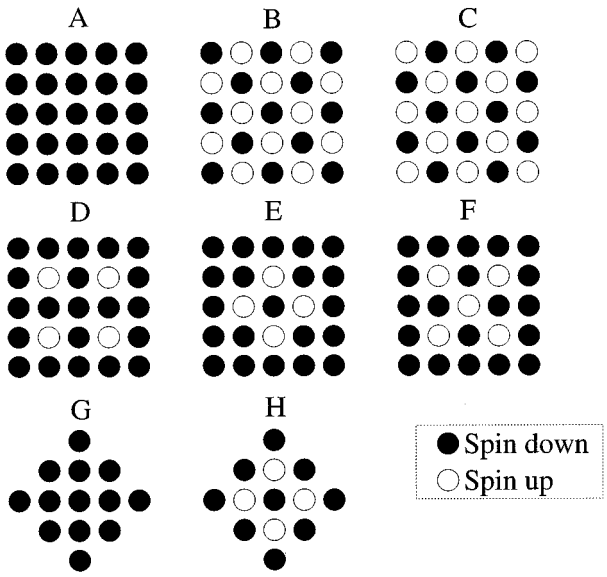

FIG. 5. Investigated magnetic configurations for square and diamond 2D Cr clusters deposited on Fe(001). A and G are $p(1\times1)^{\downarrow}$, B, C, and H are $c(2\times2)$, D is $p(2\times2)^{\downarrow}$ and, E and F are hybrid magnetic configurations. For an odd number of adatoms, there are two possibilities for $c(2\times2)$ (B and C) and hybrid (E and F) configurations. One can easily verify that the analytical expressions derived from the Ising formalism correspond to the mean of the energies obtained for the two possible configurations.

TABLE III. Total-energy differences between $p(1\times1)^{\downarrow}$ and $c(2\times2)$, $p(2\times2)^{\downarrow}$, hybrid (square) or $c2\times2$ (diamond) magnetic configuration within the Ising model. The uppercase letters correspond to the magnetic configurations represented in Fig. 2. For an odd number of adatoms, the difference is calculated between the $p(1\times1)^{\downarrow}$ total energy and the mean of the B and C (E and F) total energies in the case of a square $c(2\times2)$ (hybrid) configurations.

Config.	$\delta E = E[p(1\times1)^{\downarrow}] - E(\text{config.})$
Square $c(2\times2)(B,C)$	$4(J_1-J_2)x^2+4(2J_1-J_2)x+4J_1$
Square $p(2\times2)^{\downarrow}(D)$	$2(J_1-J_2-J_3)x^2$
Square hybrid (E,F)	$4(J_1-J_2)x^2+8(J_2-J_1-J_3)x$ $+4(J_1-J_2+3J_3)$
Diamond $c(2\times2)(H)$	$4(J_1-J_2)x^2$

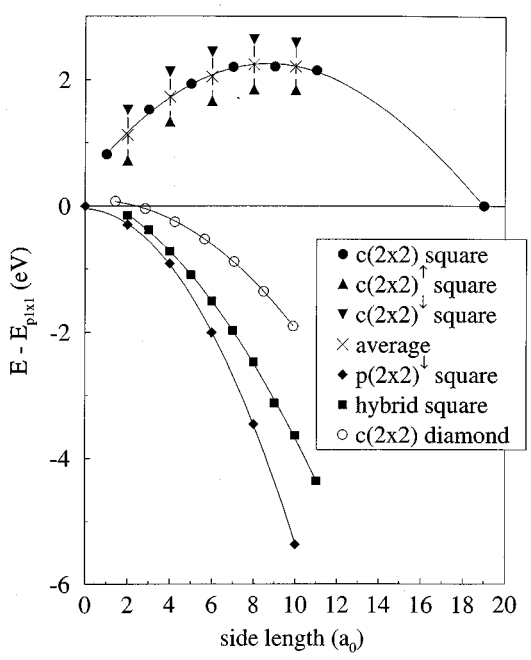

FIG. 6. Total-energy differences in meV between $p(1\times1)^{\downarrow}$ and three other configurations [$c(2\times2)$, $p(2\times2)^{\downarrow}$, hybrid] versus the cluster size x, x is measured in lattice parameter a_0 unit. The symbols show the results calculated with the tight-binding model and the curves are quadratic fits. Triangles up and down correspond to the two possible $c(2\times2)$ magnetic configurations for clusters made of an odd number of adatoms and crosses show the arithmetical mean. Note that hybrid and $p(2\times2)^{\downarrow}$ magnetic configurations are always energetically lower than the $p(1\times1)^{\downarrow}$ one whereas we must consider 20×20 adatoms cluster ($x=19$) in order to get the transition between $p(1\times1)^{\downarrow}$ and $c(2\times2)$.

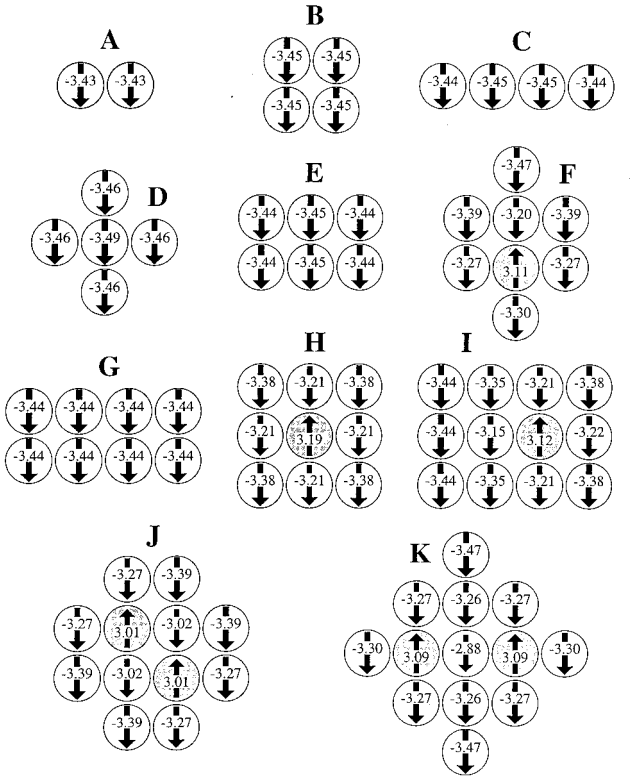

FIG. 7. Magnetic moments in μ_B of the most stable state of different clusters of Cr deposited on Fe(001). The white circles shows negative moments (nonfrustrated) and the gray circles the positive ones (frustrated). The arrows length is proportional to the moment value.

trends predicted at the end of Sec. III. The uncertainty on such quantities is estimated to be of the order of 5 meV/atom.

For cluster size larger than 6×6, we recover monolayer magnetic behavior for central adatoms. The usual coordination rule[39,41] for ferromagnetism stating that when the coordination is smaller then the moment is larger, works very nicely. For a 8×8 $p(1\times1)^{\downarrow}$ square cluster, the side adatoms moment is equal to $-3.38\mu_B$ and the edge adatoms moment to $-3.43\mu_B$. The $c(2\times2)$ case is more interesting since in this configuration, there are frustrated adatoms located on the sides and on the edges of the cluster. For nonfrustrated adatoms, the coordination rule remains valid. However, in general, the frustrated adatoms carry smaller magnetic moments if they are less coordinated. We observe similar behavior for $p(2\times2)^{\downarrow}$ and hybrid magnetic configurations.

V. SMALL CLUSTERS

In order to complete this study, we investigated a large number of small Cr clusters deposited on Fe(001) with both different geometries and magnetic configurations. Although self-consistent tight-binding calculations are done in an easier way than *ab initio* ones, the investigation of all the possibilities is out of reach. To go beyond this limitation, we tried also to use the Ising model to get easily the most stable states. The magnetic moments do not vary strongly[23] with the clusters size so that we can assume they are constant as a first approximation. In this section and as a first step, we investigate a large number of configurations both within the tight-binding model and the Ising model. Then, in the second step, all the magnetic configurations of compact clusters made of less than 25 adatoms are systematically considered and Monte Carlo studies allowing us to obtain the magnetic ground states are done for larger sizes.

Figure 7 shows the most stable states for some cluster shapes as calculated from the tight-binding model. As expected, very small clusters are in-plane ferromagnetic. However, since the geometry allows us to find central adatoms (F,H-K), the clusters recover hybrid (H-I) and even the $p(2\times2)$ (K) magnetic configurations. We considered a lot of magnetic configurations for clusters with larger sizes but we always found for the ground state either the $p(2\times2)$ if possible or the hybrid one.

On the other hand, we performed Ising calculations for all the possible magnetic arrangements and for various geometries. We used the Ising parameters derived in Secs. III and IV, and we compare the results with the previous ones we obtained with self-consistent electronic-structure calculations. The most stable states are found to be the same in both cases, except for the five adatoms cluster. For this cluster, the self-consistent calculations predict a $p(1\times1)^{\downarrow}$ (D of Fig. 7) whereas the Ising model predicts a $c(2\times2)$ (central adatoms with spin-up) configuration. However, the energy differences are very small and of the order of the uncertainty due to the

Ising parameters fit on the tight-binding results. We also compare the energy difference between magnetic configurations for both models. If a good agreement is obtained for the majority of the magnetic configurations, there are some cases for which the Ising calculations deviates strongly from tight-binding results. An accurate examination of these cases reveals that these configurations always include in-plane first neighbor frustrated adatoms coupled F with the substrate, the discrepancy being proportional to the number of these ''bad'' bonds. The energy differences between tight-binding and Ising calculations increase nearly linearly with their number, about 200 meV/bond. To understand this effect, we must take into account the fact that, from electronic-structure calculations, F bonds between frustrated and nonfrustrated adatoms are nonequivalent. In the Ising formalism, this can be obtained by adding further terms, such as $J\mathbf{S}_i^Y\mathbf{S}_j^X\mathbf{S}_k^X$. Three different in-plane first-neighbor interactions must be introduced: J_2^+ for two adatoms coupled F between themselves and coupled F with the Fe substrate, J_2^- for two adatoms coupled F and coupled AF with the substrate, and J_2^{+-} for these that are AF coupled between themselves. It is very difficult to accurately calculate these new parameters. We estimate that $J_2^- \simeq -J_2^{+-}$, assuming that J_2^- and J_2^{+-} play the same role as J_2. Then J_2^+ is found to be positive, the interaction between two adatoms coupled F and coupled AF with the substrate lowering the magnetic energy. This simple improvement of the Ising model allows a better description of the configurations presenting magnetic couplings between frustrated adatoms.

VI. SUMMARY AND OUTLOOK

Tight-binding self-consistent calculations for various magnetic configurations of transition-metal monolayers adsorbed on Fe(001) have been presented. In this framework, we have shown that neither the $p(1\times1)$ ferromagnetic nor the $c(2\times2)$ in-plane antiferromagnetic configurations are the most stable states.[1,–3,6] We propose a magnetic solution, the $p(2\times2)$ one, which we found to be lower in energy of 27 meV per adatom than the $c(2\times2)$ one. In order to understand the role of the Fe substrate, we investigate all these magnetic configurations for different 3*d* transition metals. These results confirm that a Mn monolayer deposited on Fe(001) is $c(2\times2)$ antiferromagnetic[36] and that the $p(1\times1)$ structure is the ground state for V, Ni, and Co monolayers on Fe(001). An Ising model is used to understand qualitatively the ground states. Its parameters are deduced from the self-consistent calculations. We found that the in-plane first- and second-neighbor interactions decrease from V to Ni. Moreover, the monolayer-substrate coupling is found to be strongly AF at the beginning of the series (V), weak in the middle (Mn,Fe), and strongly F at the end (Ni).

In a second part, we investigated the magnetic transitions between the $p(1\times1)$ and other magnetic states when we increase the sizes of different Cr clusters deposited on Fe(001). These calculations allowed us to determine more precisely the Ising parameters. Hence we compare Ising and tight-binding calculations that we did for small clusters with different shapes and various magnetic configurations. We found that it is necessary to upgrade the Ising model to take into account some particular cases but that in general, the agreement is very good for solutions with low energy.

Ab initio calculations are in progress to confirm the $p(2\times2)$ solution for one Cr monolayer deposited on Fe(001). Experimental confirmations are also expected. We think that the Ising formalism, despite its intrinsic simplicity, may be of great interest for studying magnetic properties of metals such as Mn and Fe.

[1] R. H. Victora and L. M. Falicov, Phys. Rev. B **31**, 7335 (1985).
[2] C. L. Fu, A. J. Freeman, and T. Oguchi, Phys. Rev. Lett. **54**, 2700 (1985).
[3] L. E. Klebanoff, R. H. Victora, L. M. Falicov, and D. A. Shirley, Phys. Rev. B **32**, 1997 (1985).
[4] A. Vega, C. Demangeat, H. Dreyssé, and A. Chouairi, Phys. Rev. B **51**, 11 546 (1995).
[5] D. Stoeffler and F. Gautier, J. Magn. Magn. Mater. **147**, 260 (1995).
[6] A. Vega, S. Bouarab, H. Dreyssé, and C. Demangeat, Thin Solid Films **275**, 103 (1996).
[7] C. Carbone and S. F. Alvarado, Phys. Rev. B **36**, 2433 (1987).
[8] R. Jungblut, C. Roth, F. U. Hillebrecht, and E. Kisker, J. Appl. Phys. **70**, 5923 (1991).
[9] T. G. Walker, A. W. Pang, H. Hopster, and S. F. Alvarado, Phys. Rev. Lett. **69**, 1121 (1992).
[10] J. Unguris, R. J. Celotta, and D. T. Pierce, Phys. Rev. Lett. **69**, 1125 (1992).
[11] Y. U. Idzerda *et al.*, Phys. Rev. B **48**, 4144 (1993).
[12] C. Turtur and G. Bayreuther, Phys. Rev. Lett. **72**, 1557 (1994).
[13] S. Miethaner, Ph.D. thesis, Universität Regensburg, 1994.
[14] S. Miethaner and G. Bayreuther, J. Magn. Magn. Mater. **148**, 42 (1995).
[15] G. Allan, Phys. Rev. B **19**, 4774 (1979).
[16] A. Werner, A. Arrott, and H. Kendrick, Phys. Rev. **155**, 528 (1967).
[17] R. Wiesendanger *et al.*, Phys. Rev. Lett. **65**, 247 (1990).
[18] L. E. Klebanoff, S. W. Robey, G. Liu, and D. A. Shirley, Phys. Rev. B **30**, 1048 (1984).
[19] C. L. Fu and A. J. Freeman, Phys. Rev. B **33**, 1755 (1986).
[20] B. Mpassi-Mabiala, H. Nait-Laziz, S. Bouarab, and C. Demangeat, J. Magn. Magn. Mater. **129**, 200 (1994).
[21] S. Blügel, M. Weinert, and P. H. Dederichs, Phys. Rev. Lett. **60**, 1077 (1988).
[22] S. Blügel, D. Pescia, and P. H. Dederichs, Phys. Rev. B **39**, 1392 (1989)
[23] K. Wildberger *et al.*, Phys. Rev. Lett. **75**, 509 (1995).
[24] O. Eriksson, G. W. Fernando, R. C. Albers, and A. M. Boring, Solid State Commun. **78**, 801 (1991).
[25] S. Ohnishi, A. J. Freeman, and M. Weinert, Phys. Rev. B **28**, 6741 (1983).
[26] V. S. Stepanyuk *et al.*, Phys. Rev. B **53**, 2121 (1996).
[27] N. W. Ashcroft and N. D. Mermin, *Solid State Physics* (Saunders College, Philadelphia, 1976).
[28] H. Shiba, Prog. Theor. Phys. **46**, 77 (1971).
[29] *The Recursion Method and Its Applications*, edited by D. G. Pet-

tifor and D. L. Weaire, Vol. 58 of *Springer Series in Solid-State Sciences* (Springer-Verlag, Berlin, 1984).
[30] R. Haydock, V. Heine, and M. J. Kelly, J. Phys. C **5**, 2845 (1972).
[31] R. Haydock, V. Heine, and M. J. Kelly, J. Phys. C **8**, 2591 (1975).
[32] N. Beer and D. G. Pettifor, in *The Electronic Structure of Complex Systems*, Vol. 113 of *NATO ASI Series B: Physics*, edited by P. Phariseau and W. M. Temmerman (Plenum, New York, 1984), p. 769.
[33] F. Ducastelle, *Order and Phase Stability in Alloys, Cohesion and Structure* (North-Holland, Amsterdam, 1991), Vol. 3.
[34] A. Vega *et al.*, Phys. Rev. B **48**, 985 (1993).
[35] S. Bouarab, M. A. Khan, and C. Demangeat, Solid State Commun. **94**, 135 (1995).
[36] R. Wu and A. J. Freeman, Phys. Rev. B **51**, 17 131 (1995).
[37] L. Pizzagalli *et al.*, J. Appl. Phys. **79**, 5834 (1995).
[38] S. Bouarab *et al.*, Phys. Rev. B **52**, 10 127 (1995).
[39] A. Vega *et al.*, J. Magn. Magn. Mater. **104-107**, 1687 (1992).
[40] A. A. Ostroukhov, V. M. Floka, V. T. Cherepin, and V. N. Tomilenko, J. Magn. Magn. Mater. **147**, 205 (1995).
[41] H. Nait-Laziz, C. Demangeat, and A. Mokrani, J. Magn. Magn. Mater. **121**, 123 (1993).